

# Anomalous Critical Slowdown at a First Order Phase Transition in Single Polymer Chains

Shuangshuang Zhang,<sup>1,2</sup> Shuanhu Qi,<sup>3,\*</sup> Leonid I. Klushin,<sup>4</sup>  
Alexander M. Skvortsov,<sup>5</sup> Dadong Yan,<sup>1</sup> and Friederike Schmid<sup>3</sup>

<sup>1</sup>*Department of Physics, Beijing Normal University, Beijing 100875, China*

<sup>2</sup>*Graduate School Of Excellence Materials Science in Mainz, Staudingerweg 9, D-55128 Mainz, Germany*

<sup>3</sup>*Institut für Physik, Johannes Gutenberg-Universität Mainz, Staudingerweg 9, D-55099 Mainz, Germany*

<sup>4</sup>*Department of Physics, American University of Beirut, P. O. Box 11-0236,  
Beirut 1107 2020, Lebanon, and Institute of Macromolecular Compounds,*

*Russian Acad. Sci. Bolshoy 31, 199004 St. Petersburg, Russia*

<sup>5</sup>*Chemical-Pharmaceutical Academy, Professora Popova 14, 197022 St. Petersburg, Russia*

Using Brownian Dynamics, we study the dynamical behavior of a polymer grafted onto an adhesive surface close to the mechanically induced adsorption-stretching transition. Even though the transition is first order, (in the infinite chain length limit, the stretching degree of the chain jumps discontinuously), the characteristic relaxation time is found to grow according to a power law as the transition point is approached. We present a dynamic effective interface model which reproduces these observations and provides an excellent quantitative description of the simulations data. The generic nature of the theoretical model suggests that the unconventional mixing of features that are characteristic for first-order transitions (a jump in an order parameter) and features that are characteristic of critical points (anomalous slowdown) may be a common phenomenon in force-driven phase transitions of macromolecules.

## A. Introduction

Phase transitions have been recognized to be among the most fascinating phenomena in physics since the days of van der Waals, Boltzmann, and Gibbs [1, 2]. In recent years, (pseudo)phase transitions in molecules have received increasing attention in biophysics and materials science, as they provide the physical basis for important biological processes [3–8] and can be exploited for nanomaterial design [9–14]. The interest in single macromolecules is also spurred by advances in experimental techniques [15, 16], which facilitate the manipulation of single molecules.

Phase-transition-like phenomena at the single molecule level often have unusual features [17, 18]. The so-called “adsorption-stretching” transition is a noticeable example, where an end-grafted chain initially adsorbed onto an adhesive surface desorbs due to a tension force acting on the free end. Analytical theory and Monte Carlo simulations have shown that this transition is first order, but nevertheless displays features that are typically associated with continuous phase transitions. In the limit of infinite chain length, the order parameter (the height of the free end) jumps discontinuously, and the heat capacity has a delta-function-like singularity, indicating that the transition is first order. However, the distribution of the order parameter is always unimodal and there are no metastable states [19, 20]. Furthermore, analytical theory predicts that the order parameter fluctuations should show an anomalous, power-like pre-transitional growth [21]. These features are typical of a second order transi-

tion.

The presence of large fluctuations at the adsorption-stretching transition point suggests that the relaxational dynamics for single macromolecules might slow down accordingly. Dynamical slowdown is common close to second order phase transitions, such as, e.g., driven desorption transition of free polymer chains on adhesive substrates [22, 23], but it would be rather untypical close to a first order transition. It should have a severe impact on the kinetics of processes that rely on mechanically driven desorption transitions.

The purpose of the present work is to present a systematic study of the static and dynamic behavior in such a system. We use Brownian dynamics (BD) simulations to investigate a single polymer chain grafted onto an adhesive surface in the vicinity of its adsorption-stretching transition point. The model does not account for hydrodynamic and entanglement effects, but it does capture the essential physics of the transition. Our simulations confirm the predicted increase of order parameter fluctuations at the transition and show that the relaxation dynamics close to the transition point slows down anomalously according to a power law. To our best knowledge, this is the first time that critical slowdown was observed at a first order phase transition in dynamical simulations. Furthermore, we present a simple effective model that captures both the static and dynamic properties of this unusual phase transition and may help to understand other, similar, molecular phase transitions.

---

\* qish@uni-mainz.de

## I. MODEL DESCRIPTION AND BROWNIAN DYNAMICS

We consider a coarse-grained polymer chain of  $N$  beads connected via Gaussian springs. One end of the chain is grafted to an impenetrable substrate located at  $z = 0$ , which otherwise imposes an attractive potential on all polymer beads. We use periodic boundary conditions along the  $x$  and  $y$  directions and impenetrable boundaries at  $z = 0$  and  $z = L_z$  in a simulation box of size  $L_x = L_y = 4\sqrt{N}$  and  $L_z = N$ . Here and throughout this paper, lengths are expressed in units of the statistical segment length  $a$ , energies in units of  $k_B T$ , and times in units of  $\zeta_0 a^2$ , where  $\zeta_0$  is the friction coefficient for each bead. In these units, the Hamiltonian of the system in a discretized form is given by

$$\mathcal{H} = \frac{3}{2} \sum_{j=2}^N (\mathbf{R}_j - \mathbf{R}_{j-1})^2 + \frac{v}{2} \sum_{\alpha} \hat{\rho}_{\alpha}^2 - F Z_1 + \sum_{j=1}^{N-1} U_a(Z_j), \quad (1)$$

in which  $\alpha$  denotes the indexes of mesh points. The four terms represent the elastic energy, the pairwise excluded volume interactions, the potential energy associated with the end force, and the attractive interaction with the substrate, respectively. Here  $\mathbf{R}_j$  denotes the location of the  $j$ th bead,  $Z_j$  the corresponding  $z$ -component (with  $Z_N = 0$ ), and non-bonded interactions are formulated in terms of the bead density operator  $\hat{\rho}_{\alpha} = \hat{\rho}(\mathbf{r}_{\alpha}) = \frac{1}{\Delta V} \sum_j g(|\mathbf{R}_j - \mathbf{r}_{\alpha}|)$  [24, 25], and  $\Delta V$  is the volume of one mesh cell,  $g$  being an assignment function depending on the distance between the bead and the mesh point. We choose the function  $g$  such that the fraction assigned to a given mesh point is proportional to the volume of a rectangle whose diagonal is the line connecting the particle position and the mesh point on the opposite side of the mesh cell. This is the so called Cloud-in-Cells (CIC) scheme [26–28]. We set the cloud/cell size  $\Delta V = 1$  and  $z$ -components of vortices located at  $z = 0.5 + m$  ( $m \in \mathbb{N}$ ). To simplify the notation for the coordinate of the free end which is one of the main quantities of interest, in the rest of the paper we drop the subscript:  $Z = Z_1$ . The excluded volume parameter  $v$  is set to  $v = 1$  such that the grafted polymer is in good (implicit) solvent. The surface interaction potential is defined through  $U_a(\mathbf{r}) = -\varepsilon \min(1, 3/2 - z)$  for  $0 \leq z \leq 3/2$ , and  $U_a(\mathbf{r}) = 0$  otherwise. Here,  $\varepsilon > 0$  is the energy gain if a monomer is in contact with the substrate. Thus the potential equals  $-\varepsilon$  at  $0 \leq z \leq 1/2$ , and then linearly approaches zero at  $z = 3/2$ . We note that  $\mathcal{H}$  is a continuous function of the bead positions  $\mathbf{R}_j$ , since the density operator  $\hat{\rho}(\mathbf{r})$  is a continuous function of the  $\mathbf{R}_j$ . The bead positions evolve according to the equations of overdamped Brownian dynamics,  $\dot{\mathbf{R}}_j = -\partial \mathcal{H} / \partial \mathbf{R}_j + \sqrt{2} \mathbf{f}_r$ , where  $\mathbf{f}_r$  is an uncorrelated and Gaussian distributed random force with mean zero and variance  $\langle f_{r\alpha}(t) f_{r\beta}(t') \rangle = \delta_{\alpha\beta} \delta(t - t')$  ( $\alpha, \beta = x, y, z$ ). The time step in the simulation is chosen  $\delta t = 0.005$ . Quantities of interest are extracted from the trajectories of the free end bead  $j = 1$ . For details of the

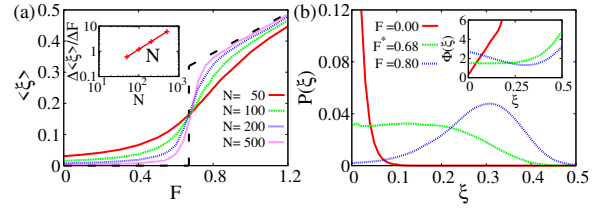


FIG. 1. (a) Stretching degree  $\langle \xi \rangle$  as a function of stretching force  $F$  for chain lengths  $N = 50, 100, 200, 500$  at adsorption strength  $-\varepsilon = 0.80$ . The dashed line represents the asymptotic limit  $N \rightarrow \infty$ . The inset shows the maximum slope, which is proportional to  $N$ . (b) Probability distribution of the order parameter  $\xi$  at chain length  $N = 100$  in the adsorbed state  $F = 0.00$ , at the transition point  $F^* = 0.68$ , and in the stretched state  $F = 0.80$ . Inset shows the corresponding Landau free energy curves  $\Phi(\xi)$ .

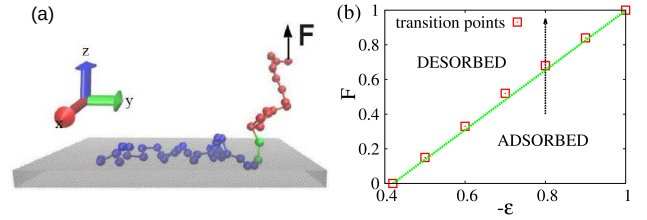


FIG. 2. (a) Snapshot from BD simulation of the polymer chain at the transition point ( $-\varepsilon = 0.80, F = 0.68$ ), where the probability distribution  $P(\xi)$  exhibits a broad plateau. The gray region represents the attractive surface layer. Blue beads are adsorbed, red ones belong to stretched chain parts, and green ones are at the interface between these two states. (b) Critical tensile force  $F^*$  as a function of surface potential strength  $\varepsilon$ , which obeys a power law  $F^* \propto (|\varepsilon| - |\varepsilon_c|)^x$  with  $\varepsilon_c = -0.42 \pm 0.02$ , and  $x = 1.0 \pm 0.03$  (green line).

BD simulation scheme, we refer to the Supplementary material.

## II. CHARACTERIZATION OF THE PHASE TRANSITIONS

We begin with identifying the order of the transition by examining the conformational properties of the single chain, which can be characterized by the distribution of the free end. Specifically, we choose the stretching degree  $\xi = Z/N$  as the order parameter, where  $Z$  is the distance between the free end and the substrate. Fig. 1(a) shows the profiles of the mean order parameter  $\langle \xi \rangle$  as a function of the control parameter, the pulling force  $F$ , at adsorption strength  $-\varepsilon = 0.8$  for several finite chain lengths. Here  $\langle \cdots \rangle$  denotes ensemble averages. The curves of different  $N$  intersect at almost the same point, which hence identifies the transition force  $F^*$ . In the vicinity of the transition, the profile become sharper with increasing  $N$ . The maximum slope of each curve increases linearly with increasing  $N$  Fig. 1(a), inset). Hence, in the limit of

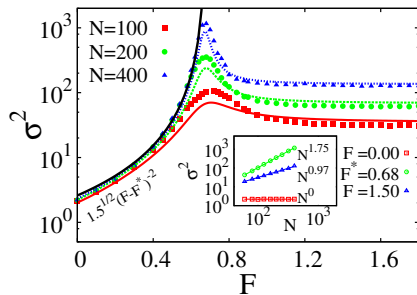


FIG. 3. Fluctuations  $\sigma^2$  of the free end position  $Z$  vs stretching force  $F$  for chain lengths  $N = 100, 200, 400$  at adsorption strength  $-\varepsilon = 0.80$ . Symbols are simulation data, lines correspond to the analytical prediction, Eqs. (5-7). The thick black line indicates the asymptotic power law divergence  $(F-F^*)^{-2}$  upon approaching  $F^*$  from the adsorbed state. Inset shows scaling of  $\sigma^2$  with  $N$  in the adsorbed state ( $F = 0$ ), at the transition ( $F = F^*$ ), and in the stretched state ( $F = 1.5$ ).

$N \rightarrow \infty$ , a discontinuous abrupt jump of  $\langle \xi \rangle$  at the transition point can be expected (see the dashed line in Fig. 1(a)). This is a clear signal of a first order transition, which is smoothed in simulations due to the finite chain lengths.

However, the order parameter distribution  $P(\xi)$ , shown in Fig. 1(b), features a single broad peak at the transition point  $F^* = 0.68$  and not a double peak structure as one would expect for a first order transition. These observations are consistent with theoretical predictions for ideal non-reversal random walks [19] and for self-avoiding chains [20] as well as with simulation results for spring-bead chains with hard core interactions [20]. The corresponding Landau free energy, which is defined as  $\Phi(\xi) = -\ln P(\xi)$ , has only one minimum, there are no metastable states (Fig. 1 (b), inset). At the transition, the Landau free energy has a wide plateau region stretching from  $\xi = 0$  to  $\xi \sim 0.2$ , and there is no sign of an energy barrier between coexisting adsorbed and stretched states. This can be explained from the fact that in this single-chain system, the interface between stretched and adsorbed chain sections comprises only a few monomers (see Fig. 2(a)), hence the interfacial free energies are negligibly small.

The phase diagram of the system is shown in Fig. 2(b) in the plane of stretching force  $F$  vs. adsorption strength  $(-\varepsilon)$ . A line of order transitions  $F^*(\varepsilon)$  separates the desorbed state from the adsorbed state, which ends in a critical point at  $(F^*, \varepsilon) = (0, \varepsilon_c)$  with  $\varepsilon_c = 0.42 \pm 0.02$ . This point corresponds to the thermodynamically driven adsorption transition, which is governed by the competition between the attractive adsorption energy and the conformational entropy loss for polymer chains near the impenetrable wall. The critical adsorption point by definition refers to the thermodynamic limit  $N \rightarrow \infty$ , and in this limit does not depend on whether the chain is grafted or not. The first order desorption line roughly follows  $F^* \propto (|\varepsilon| - |\varepsilon_c|)^x$  with  $x = 1.00 \pm 0.03$ .

Next we examine the static behavior of the chain if the transition line is crossed at fixed adsorption strength. We set  $-\varepsilon = 0.80$  (following the black dashed arrow in Fig. 2(b)), and investigate the behavior of the free end fluctuation normal to the substrate,  $\sigma^2 \equiv \langle Z^2 \rangle - \langle Z \rangle^2$ . Fig. 3 displays  $\sigma^2$  as a function of the stretching force  $F$ . In the adsorbed state, when the stretching force is small ( $F < 0.5$ ),  $\sigma^2$  is largely independent of the chain length and increases monotonically with increasing  $F$ . In the stretched state at large  $F$ ,  $F > 1.2$ ,  $\sigma^2$  is almost independent of  $F$ , but increases linearly with the chain length. It roughly obeys  $\sigma^2 \approx N/3$ , which is the behavior of a deformed Gaussian coil. The BD model we utilize here does not include the finite extensibility effect, as seen from the Hamiltonian of Eq.(1). Thus the fluctuations become Gaussian fluctuation at strong forces when the excluded volume effects become negligible. As the transition point is approached from below,  $\sigma^2$  first increases sharply and then saturates at a finite value due to the finite chain length. The extremely large values of  $\sigma^2$  at the transition point simply reflect the fact that the chain can assume adsorbed, stretched, and intermediate states with almost equal probability. However, the behavior of  $\sigma^2$  upon approaching the transition point is unconventional. Usually, fluctuations exhibit a  $\delta$ -peak at first order transitions, and power law divergences at second order transitions. Here the phase transition is first order, but the fluctuations nevertheless diverge according to a power law,  $\sigma^2 \sim \frac{1}{(F-F^*)^2}$ , independent of chain length. The divergence is cut off at  $F^*$  due to the finite length of the chains. This is analogous to the behavior predicted analytically for ideal chains [21, 29]. Right at the transition,  $\sigma^2$  was predicted to scale as  $\sigma^2 \propto N^2$  with the chain length [19–21], which is also in rough agreement with our simulation results ( $\sigma^2 \propto N^{1.75}$  according to Fig. 3, inset). The absolute value of  $\sigma^2$  at the transition is slightly underestimated by the theory. This is because the theory is based on an ideal chain model, and in real chains, the fluctuations are further enhanced due to excluded volume interactions.

### III. EFFECTIVE INTERFACE MODEL

Based on the observations above, we will now develop a simple model which gives insight into the physical origin of the anomalous behavior at this molecular phase transition, and which will provide a starting point for discussing the dynamical properties at the transition. Let us first examine once more the snapshot of a chain at the transition point, shown in Fig. 2(a). An adsorbed and a stretched block coexist within the same molecule. The interfacial region connecting the two blocks consists of only one or two segments (marked green), hence the excess energy required for creating the interface is close to negligible. Nevertheless, it is important to note that at most *one* such interface can exist in the system. This is because the stretching force acting on the chain end

is transmitted along the stretched block up to the “interface”, i.e., the first contact with the surface, and then transferred to the substrate. It does not directly influence the conformations of the adsorbed block. This distinguishes the present system from conventional one dimensional systems such as the one dimensional Ising model, where phase transitions are suppressed because they are filled with many interfaces. Here, we have only one interface separating the stretched and adsorbed block, which is free to move along the chain.

This motivates the construction of a dynamic effective interface model, which describes the system in terms of the position  $n$  of the interface within the chain. Here  $n$  is the label of the segment that establishes the first contact with the substrate, counted from the free end: thus it has the meaning of the tail length. The interface is close to the graft point ( $n \rightarrow N$ ) in the stretched state and close to the end point ( $n \rightarrow 1$ ) in the adsorbed state, and at the transition, it moves abruptly from one end to the other. The corresponding effective interface Hamiltonian has the following generic form:

$$\mathcal{H}_{\text{eff}}(n) = V_l(n) + V_r(N - n) - \delta n, \quad (2)$$

where  $\delta \propto (F - F^*)$  is the difference between the adsorption and the stretching free energies per monomer, while  $V_l(n)$  and  $V_r(n)$  are the left and right repulsive potentials which ensure that  $n$  stays within its bounds ( $0 < n < N$ ). A hard-wall boundary is nearly exact for a strong pulling force whereby the stretched tail is not affected directly by the presence of an impenetrable substrate. However, it has a disadvantage that the minimum always resides at one of the boundaries which does not allow for a simple analytical treatment of the dynamic behavior. We utilize instead a symmetric weakly diverging logarithmic potential,  $V_l(n) = V_r(n) = -A \log(n)$ , where  $A$  is a numerical prefactor, leading to a very similar behavior at large  $N$  with the benefit of generating a smooth minimum. In order to put further discussion on a quantitative basis we choose the value of  $A$  to obtain the best match with the hard boundary model and with the known results of the more sophisticated statistical theory [19–21]. The minimum of  $\mathcal{H}_{\text{eff}}(n)$  defines the most probable tail length and is attained at

$$\bar{n} = N \left( \frac{1}{2} - \frac{A}{N\delta} \pm \sqrt{\frac{1}{4} + \left( \frac{A}{N\delta} \right)^2} \right). \quad (3)$$

which has two branches, i.e., the positive and negative branch defined by the sign before the square root term. In the pre-transition region where  $\delta < 0$ , we take the negative branch, while in the post-transition region where  $\delta > 0$ , we take the positive branch. At  $\delta = 0$ , we have  $\bar{n} = N/2$ . The most probable tail length obtained in the large  $N|\delta|$  limit is  $\bar{n} = N - A/\delta$  for  $N\delta \gg 1$ , and it is  $\bar{n} = -A/\delta$  for  $N\delta \ll -1$ . It is clear that  $\bar{n}(\delta)$  approaches a step function in the limit  $N \rightarrow \infty$ ,  $\bar{n} = N\Theta(\delta)$  leading to the observed jump in the order parameter characteristic of the first-order transition. The fluctuation of  $n$

about  $\bar{n}$  are evaluated as

$$\sigma_n^2 = (V_l''(\bar{n}) + V_r''(N - \bar{n}))^{-1} = \frac{1}{A} \frac{\bar{n}^2(N - \bar{n})^2}{\bar{n}^2 + (N - \bar{n})^2}. \quad (4)$$

The maximum fluctuations are obtained at the transition point,  $\delta = 0$ , with  $\bar{n} = N/2$  and  $\sigma_n^2 = \frac{N^2}{8A}$ , while far from the transition point,  $N|\delta| \gg 1$ , the fluctuations decay as  $\sigma_n^2 \simeq \frac{A}{\delta^2}$ . On the other hand, the corresponding fluctuations for the hard boundary model are  $\sigma_n^2 = \frac{N^2}{12}$  at  $\delta = 0$  and  $\sigma_n^2 \simeq \frac{1}{\delta^2}$  for  $N|\delta| \gg 1$ , see Supplementary material. It is clear that the choice of  $A = 3/2$  fixes the correct value of fluctuations at maximum, while  $A = 1$  properly represents behavior away from the transition. To provide for the overall best match we choose the geometric mean value  $A = \sqrt{3/2}$  hereafter.

To calculate the fluctuations  $\sigma^2$  of the end position shown in Fig. 3, we must combine these results with the statistical properties of the desorbed tail. We assume that excluded volume effects are suppressed by stretching and describe the stretched tail as a deformed Gaussian coil of  $n$  segments, hence the end position  $Z$  is Gaussian distributed with mean  $\bar{Z}_1(n) = nF/3$  and variance  $\sigma_c^2(n) = n/3$ . With these assumptions, the full expression for the end fluctuations contains two contributions,

$$\sigma^2(Z) = \sigma_1^2(Z) + \sigma_2^2(Z) \quad (5)$$

the first one describing the end fluctuations of the tail at the fixed (most probable) tail length,  $\sigma_1^2(Z) = \bar{n}/3$ , and the second  $\sigma_2^2 = \sigma_n^2 F^2/9$  being proportionate to the fluctuations of the boundary. Expressions for the two terms of Eq. 5 must be corrected for small forces since the properties of the desorbed tail are then strongly affected by the presence of the wall. We do this in an *ad hoc* way to match the known behavior at  $F = 0$ . Namely, the first term is amended by adding an  $F$ -independent constant

$$\sigma_1^2(Z) = \frac{\bar{n}}{3} + \bar{n}_0 \left( \frac{4 - \pi}{6} - \frac{1}{3} \right), \quad (6)$$

where  $\bar{n}_0 = \bar{n}|_{F=0}$ , so that at zero force the fluctuations of an ideal mushroom are described correctly. It is clear that the second term,  $\sigma_2^2(Z) = \sigma_n^2 F^2/9$ , vanishes at  $F = 0$ . This underestimates the effect of  $n$  fluctuations since the mean end height in the mushroom state never turns to 0. The correct value of the second term at  $F = 0$  can be inferred from the theory [19–21], and the amended expression interpolates between the two limits of large and vanishing force

$$\sigma_2^2(Z) = \sigma_n^2 \left[ \frac{F^2}{9} + \frac{\pi - 2}{6\bar{n}_0} \exp \left( -\frac{\bar{n}F^2}{6} \right) \right]. \quad (7)$$

Here the interpolation is introduced *via* an exponentially decaying weight where the exponent,  $\bar{n}F^2/6$ , represents the stretching free energy of the tail and quantifies the relative importance of the stretching effect in comparison to that of the impenetrable wall. The linearized expression for  $\delta$  is taken from the continuum ideal chain model:  $\delta = \frac{F^*(F - F^*)}{3}$  [21]



We go all this way in order to be able to utilize the effective interface model in describing the chain dynamics: accurate decomposition of total  $Z$ -fluctuations into two terms, one being related to the boundary fluctuations, and the other describing fluctuations of  $Z$  at fixed boundary position, is central to the dynamic theory. The theoretical prediction for chain end fluctuations is in good agreement with the simulation results (see Fig.(3)). This includes the power-law growth upon approaching the transition point, as well as the anomalous fluctuation  $\sigma^2 \propto \sigma_n^2 \propto N^2$  at the transition point  $\delta = 0$ , consistent with the more sophisticated statistical theory [19–21] and the data in Fig.(3). The fact that the apparent exponent at the transition point  $\sigma \propto N^{1.8}$  is slightly less than 2 reflects finite-size corrections to the dominant scaling in the explored range of  $N$ .

#### IV. DYNAMIC RELATION AND CRITICAL SLOWDOWN

We now apply the effective interface model to estimate the relaxation dynamics in our system. We suppose that the interface undergoes a random process, following a Langevin equation

$$\frac{dn}{dt} = D(n) \cdot f(n) + \sqrt{2D(n)} \eta, \quad (8)$$

where  $D(n)$  and  $f(n) = -\frac{\partial \mathcal{H}_{\text{eff}}}{\partial n}$  are the mobility and the “driving force” and  $\xi$  is a Gaussian distributed white noise with variance  $\langle \eta(t)\eta(t') \rangle = \delta(t-t')$  [30]. The inverse mobility  $D^{-1}(n)$  is governed by two contributions to the dissipation upon moving the boundary. First, there is viscous drag as the desorbed tail moves against the solvent, which scales as  $\propto N$  for free-draining chains [21, 31] and should be independent of the adsorption strength. Second, the motion of the boundary involves breaking the contact with the adsorbing surface. This source of dissipation is expected to depend on  $\varepsilon$  but not on the tail length. Altogether, we write

$$D^{-1}(n) = \alpha n \zeta_0 + \zeta_{\text{ads}}, \quad (9)$$

where  $\zeta_0$  is the translational monomer friction coefficient (in our dynamic simulation scheme  $\zeta_0$  defines the time scale and is taken as 1),  $\alpha$  is the fraction of the tail effectively involved in the boundary fluctuations, and  $\zeta_{\text{ads}}$  is the friction coefficient associated with local adsorption-desorption kinetics. A variable diffusion coefficient  $D(n)$  leads to a multiplicative noise, which can be solved by a standard transformation of variables (see Supplementary material). This has a disadvantage of involving a cubic equation for the position of the relevant minimum. To keep the analytics tractable we adopt a naive way of treating the diffusion coefficient as a constant evaluated at the most probable value of the tail length,  $D = D(\bar{n})$  where  $\bar{n}$  is given by Eq. (3).

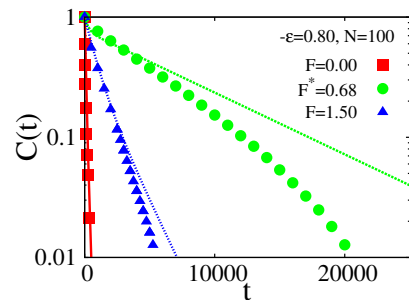


FIG. 4. Examples of time autocorrelation function  $C(t)$  of the end position for chain length  $N = 100$  at  $-\varepsilon = 0.80$  and three different stretching forces corresponding to an adsorbed state ( $F < F^*$ ), a stretched state ( $F > F^*$ ), and the transition ( $F = F^*$ ). Symbols correspond to data from BD simulations, and lines show the prediction from Eq. (11) for  $\zeta_0 = 1$ ,  $\alpha = 0.25$ , and  $\zeta_{\text{ads}} = 1.8$ .

We assume that the characteristic time scale for the motion of the boundary is dominated by the diffusive process around the minimum of  $\mathcal{H}_{\text{eff}}(n)$  at  $\bar{n}$ . Hence the evolution of  $n$  is approximated by the Ornstein-Uhlenbeck process, which has the characteristic relaxation time [32]

$$\tau_n = D^{-1}(\bar{n})\sigma_n^2. \quad (10)$$

Specifically, in the three limits  $\tau_n \propto 1/|\delta|^3$  for  $\delta < 0$  (adsorbed state),  $\tau_n \propto N/\delta^2$  for  $\delta > 0$  (stretched state), and  $\tau_n \propto N^3$  for  $\delta = 0$  (transition point).

To calculate the autocorrelation function of the end position,  $C(t) = \frac{1}{\sigma^2(Z)}(\langle Z(t)Z(0) \rangle - \langle Z \rangle^2)$ , we rewrite  $Z$  as  $Z = \bar{Z}(n(t)) + y(t)$ , where  $y(t)$  accounts for the conformational fluctuations of the desorbed tail at a fixed position of the boundary. The autocorrelation function at fixed boundary is written as  $\langle y(t)y(0) \rangle \approx \sigma_1^2 \exp(-t/\tau_R(\bar{n}))$  where  $\sigma_1^2$  is evaluated according to Eq. (6) and  $\tau_R(\bar{n})$  is the relaxation time of the end position at fixed tail length. This can be obtained as the average end-to-end distance relation time of the multi-mode Rouse model with one end fixed:  $\tau_R(\bar{n}) = \frac{1}{9}\zeta_0\bar{n}^2$  [31]. Neglecting cross-correlations we obtain

$$C(t) = \frac{1}{\sigma_1^2(Z) + \sigma_2^2(Z)} \left( \sigma_1^2(Z) e^{-t/\tau_R(\bar{n})} + \sigma_2^2(Z) e^{-t/\tau_n} \right). \quad (11)$$

where the variances  $\sigma_1^2(Z)$  and  $\sigma_2^2(Z)$  are evaluated at the most probable value  $\bar{n}$  according to Eqs.(6, 7). From  $C(t)$  we can calculate the average relaxation time [33],  $\tau = \int_0^\infty dt C(t)$ , giving

$$\tau = \frac{1}{1 + \Phi} \tau_n + \frac{\Phi}{1 + \Phi} \tau_R(\bar{n}) \quad (12)$$

where  $\Phi = \sigma_1^2(Z)/\sigma_2^2(Z)$ .

Fig. (4) compares simulation results for the autocorrelation function with the theoretical predictions for  $\alpha = 0.25$  and  $\zeta_{\text{ads}} = 1.8$  for selected parameter sets. The data are in reasonable agreement with the simulation results

at early and intermediate times. Deviations can be observed at late times especially at  $F^* = 0.68$ , where the simulation data decay faster than exponentially. In this regime, the boundary diffuses along the whole chain, and the harmonic approximation (Eq. 10) becomes questionable. However, although the differences in the figure for curves at  $F^*$  seem large, they appear mainly at late times where  $C(t)$  is small, and do not have a large effect on the average relaxation time  $\tau$  (only about 20 %).

The simulation results for the average relaxation time,  $\tau$  are shown in Fig. 5 together with the theoretical predictions (again using  $\alpha = 0.25$  and  $\zeta_{\text{ads}} = 1.8$ ). In the fully desorbed state,  $\tau$  is dominated by  $\tau_R(\bar{n})$  and proportional to  $N^2$ , and Rouse relaxation describes the strong force limit very accurately. In the adsorbed state,  $\tau$  is dominated by  $\tau_n$  and chain length independent, and it shows the predicted power law dependence as one approaches the critical stretching point. Hence we observe critical slowing down, unusual for a first order transition. Right at the transition, the relaxation times become very slow and scales as  $\tau \propto N^{2.8}$  (Fig. 5, inset), which is also close to the limiting behavior predicted by the model,  $\tau \sim \tau_n \propto N^3$ . Altogether, the dynamic model successfully captures three different regimes (adsorbed, desorbed, and near-critical) for chains of different lengths.

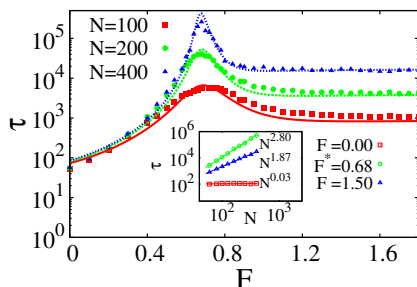


FIG. 5. Characteristic relaxation time  $\tau$  of free end correlations vs. stretching force for chain lengths  $N = 100, 200, 400$  at  $-\varepsilon = 0.80$ . Symbols are data from BD simulations, and lines correspond to the prediction based on the dynamic model. at  $\zeta_0 = 1, \alpha = 0.25$ , and  $\zeta_{\text{ads}} = 1.8$ . Inset shows scaling of  $\tau$  with  $N$  in the adsorbed state ( $F = 0$ ), at the transition ( $F = F^*$ ), and in the stretched state ( $F = 1.5$ ).

## V. SUMMARY

To summarize, we have utilized BD simulations to study the adsorption-stretching transition of a polymer chain tethered onto an adhesive solid surface, with a tension force exerted at the free chain end. Even though the transition is first order, we found critical (power-law) slowdown close to the transition point, as is typical for continuous phase transitions. Our observations could be rationalized by a simple model that describes the system in terms of single interface separating the adsorbed and

stretched chain blocks. Close to the transition, the relaxation dynamics is governed by the time scale of the interface diffusion, which diverges at the transition.

The good correspondence of the theory and simulations in the case of the dynamic properties is perhaps fortuitous, since extra fitting parameters related to friction coefficients were introduced in the theory. However, regarding the static properties, the choice of the amplitude parameter was based on comparison between hard walls and logarithmic potential which was not just a simple fitting of the final data.

In the BD simulations, we adopt a coarse-grained off-lattice model, which can be seen as the dynamic version of the off-lattice MC scheme proposed by Laradji et al (see ref.[25]). In this approach the excluded volume interactions are replaced by soft interactions that are formulated in terms of local monomer densities. Compared to the more commonly used coarse-grained models with non-bonded hard core potentials, this approach has the two advantages. First, it can be simulated very efficiently, since the most time consuming part, an explicit evaluation of the pair potentials, is avoided. Second, since it uses soft potentials, equilibrium times are comparatively short. Soft potentials account properly for the density correlations (at least on the large scales) that are characteristic of the excluded volume interactions. With such models, the static behavior of single chains (in particular, the Flory exponent) can be captured correctly. On the other hand, they do not impose the dynamic constraint that chain self-crossing is forbidden. Thus, topological effects such as entanglements or knots which may influence the dynamics strongly, are not accounted for correctly here. For single-chain dynamics in the presence of a stretching force these topological effects are typically neglected. This can be motivated by the observation that single chains in good solvents typically do not contain knots at the chain lengths considered in the present study [34]. In the presence of a stretching force, the knot probability should be further reduced. Correlated fluctuations due to excluded volume effects are important at zero (or very weak) external forces. Strong stretching generally screens out the global excluded volume effects.

In the present work, we have demonstrated anomalous dynamic slowdown in the vicinity of a first order transition. An additional source of slowdown comes into play if one approaches the critical adsorption point (the point  $\epsilon^* = -0.42, F^* = 0$  in Fig. 2). Whereas the slow dynamics in the situation discussed here is a result of the slow diffusion of an interface, critical slowdown is associated with the slow relaxation of very large loops. These phenomena will be analyzed in more detail in future work.

Our simple model might be useful also for the interpretation of other, similar, macromolecular transitions, such as, e.g., the force-induced unzipping transition of DNA or RNA [5, 35–37]. In simulations, the (nonequilibrium) transition times for unzipping were found to scale as  $N^3$  with the chain length [5], which is consistent with our

findings. We would expect that the relaxation times in the vicinity of the unzipping transition also show a critical power-law behavior. Unusual static and dynamic behavior close to macromolecular phase transitions might be ubiquitous in nature, therefore the study of such phenomena is more than just intriguing and may bring new insight in understanding biological processes.

**Supplementary material** Supporting Material contains the detailed description of the simulation scheme, a comparison of the two models (hard walls vs. logarithmic boundary potential) and the accurate treatment of

the Langevin equation for the boundary with a variable diffusion coefficient.

### Acknowledgements

This work has been supported by the German Science Foundation (DFG) within the Graduate School of Excellence Materials Science in Mainz (MAINZ), the SFB TRR 146 (project C1) and the Grant Schm 985/13-2. S.Z. acknowledges financial support from the National Science Foundation of China (NSFC) 21374011, 21434001. Simulations were carried out on the computer cluster Mogon at JGU Mainz (hpc.uni-mainz.de).

- 
- [1] H. E. Stanley, *Introduction to Phase Transitions and Critical Phenomena* (Clarendon Press, Oxford, 1971).
  - [2] J. M. Yeomans, *Statistical Mechanics of Phase Transitions* (Oxford Science Publications, 1992).
  - [3] B. Essevaz-Roulet, U. Bockelmann, and F. Heslot, *Proc. Natl. Acad. Sci.* **94**, 11935 (1997).
  - [4] U. Bockelmann, P. Thomen, B. Essevaz-Roulet, V. Viasnoff, and F. Heslot, *Biophys. J.* **82**, 1537 (2002).
  - [5] D. Marenduzzo, S. M. Bhattacharjee, A. Maritan, E. Orlandini, and F. Seno, *Phys. Rev. Lett.* **88**, 028102 (2002).
  - [6] J. Kierfeld, *Phys. Rev. Lett.* **97**, 058302 (2006).
  - [7] J. Paturej, J. L. A. Dubbeldam, V. G. Rostiashvili, A. Milchev, and T. A. Vilgis, *Soft Matter* **10**, 2785 (2014).
  - [8] J. Paturej, A. Milchev, V. G. Rostiashvili, and T. A. Vilgis, *Macromolecules* **45**, 4371 (2012).
  - [9] M. A. C. Stuart, W. T. S. Huck, J. Genzer, M. Müller, C. Ober, M. Stamm, G. B. Sukhorukov, I. Szleifer, V. V. Tsukruk, M. Urban, F. Winnik, S. Zauscher, I. Luzinov, and S. Minko, *Nat. Mater.* **9**, 101 (2010).
  - [10] T. Chen, R. Ferris, J. Zhang, R. Ducker, and S. Zauscher, *Prog. Polym. Sci.* **35**, 94 (2010).
  - [11] L. I. Klushin, A. M. Skvortsov, A. A. Polotsky, S. Qi, and F. Schmid, *Phys. Rev. Lett.* **113**, 068303 (2014).
  - [12] S. Qi, L. I. Klushin, A. M. Skvortsov, A. A. Polotsky, and F. Schmid, *Macromolecules* **48**, 3775 (2015).
  - [13] H. M. amd G.-L. He, C.-V. Wu, and J.-U. Sommer, *Macromolecules* **41**, 5070 (2008).
  - [14] D. Romeis, H. Merlitz, and J.-U. Sommer, *J. Chem. Phys.* **136**, 044903 (2012).
  - [15] M. Rief, F. Oersterhelt, B. Heymann, and H. E. Gaub, *Science* **275**, 1295 (1997).
  - [16] S. B. Smith, Y. Cui, and C. Bustamante, *Science* **271**, 795 (1996).
  - [17] L. I. Klushin and A. M. Skvortsov, *J. Phys. A: Math. Theor.* **44**, 473001 (2011).
  - [18] J. L.-Strathmann and K. Binder, *J. Chem. Phys.* **141**, 114911 (2014).
  - [19] A. M. Skvortsov, L. I. Klushin, A. A. Polotsky, and K. Binder, *Phys. Rev. E* **85**, 031803 (2012).
  - [20] S. Bhattacharya, V. G. Rostiashvili, A. Milchev, and T. A. Vilgis, *Phys. Rev. E* **79**, 030802 (2009).
  - [21] A. A. Gorbunov and A. M. Skvortsov, *J. Chem. Phys.* **98**, 5961 (1993).
  - [22] S. Granick, S. K. Kumar, E. J. Amis, M. Antonietti, A. C. Balazs, A. K. Chakraborty, G. S. Grest, C. Hawker, P. Janmey, and E. J. J. Kramer, *Polym. Sci., Part B: Polym. Phys.* **41**, 2755 (1993).
  - [23] G. J. Fleer, M. A. C. Stuart, J. M. H. M. Scheutjens, T. Cosgrove, and B. Vincent, *Polymers at interfaces* (Chapman and Hall, London, 1993).
  - [24] E. Helfand, *J. Chem. Phys.* **62**, 999 (1975).
  - [25] M. Laradji, H. Guo, and M. J. Zuckermann, *Phys. Rev. E* **49**, 3199 (1994).
  - [26] C. K. Birdsall and D. Fuss, *J. Comput. Phys.* **135**, 141 (1997).
  - [27] F. A. Detcheverry, H. Kang, K. C. Daoulas, M. Müller, P. F. Nealey, and J. J. de Pablo, *Macromolecules* **41**, 4989 (2008).
  - [28] G. Milano and T. Kawakatsu, *J. Chem. Phys.* **130**, 214106 (2009).
  - [29] The analytical theory deals with the Gaussian chain model, where the excluded volume interactions are ignored. We found that the inclusion of excluded volume interaction mainly shifts the transition point.
  - [30] C. W. Gardiner, *Handbook of Stochastic methods* (Springer-Verlag, Berlin, 2nd Ed., 1990).
  - [31] M. Doi and S. F. Edwards, *The theory of polymer dynamics* (Oxford University Press, 1999).
  - [32] H. Risken, *The Fokker-Planck Equation*, Springer Series in Synergetics, Vol. 18 (Springer, 1996).
  - [33] J. P. Hansen and I. R. McDonald, *Theory of Simple Liquids* (Academic, New York, 1986).
  - [34] P. Virnau, Y. Kantor, and M. Kardar, *J. Am. Chem. Soc.* **127**, 15102 (2005).
  - [35] M. S. Causo, B. Coluzzi, and P. Grassberger, *Phys. Rev. E* **62**, 3 (2000).
  - [36] A. M. Skvortsov, L. I. Klushin, G. J. Fleer, and F. A. M. Leermakers, *J. Chem. Phys.* **132**, 064110 (2010).
  - [37] D. K. Lubensky and D. R. Nelson, *Phys. Rev. Lett* **85**, 1572 (2000).